agronomy

MDPI

*Article*

# Investigation of Soils and Pine Needles Using WDXRF and TXRF Techniques for Assessment of the Environmental Pollution of Shelekhov District, Eastern Siberia, by the Aluminum Industry and Heat Power Engineering

**Victor Chubarov [1,*], Tatiana Cherkashina [2], Artem Maltsev [2], Elena Chuparina [1], Alena Amosova [1] and Sergey Prosekin [1]**

[1] Vinogradov Institute of Geochemistry, Siberian Branch of the Russian Academy of Sciences, Irkutsk 664033, Russia; lchup@igc.irk.ru (E.C.); amosova@igc.irk.ru (A.A.); pros.sergey@igc.irk.ru (S.P.)
[2] Institute of the Earth's Crust, Siberian Branch of the Russian Academy of Sciences, Irkutsk 664033, Russia; tcherk@crust.irk.ru (T.C.); artemmaltsev1@gmail.com (A.M.)
* Correspondence: chubarov@igc.irk.ru

**Abstract:** X-ray fluorescence analysis was applied to assess the ecological state of the area potentially polluted by emissions of the aluminum industry and heat power engineering. Soil and pine needle samples were collected in areas with industrial activity and analyzed using wavelength-dispersive X-ray fluorescence (WDXRF) and total-reflection X-ray fluorescence (TXRF) techniques. Both techniques were validated using the matrix-matched certified reference materials. Different sample preparation procedures, such as fusion and pressing for WDXRF and acid digestion and suspensions for TXRF as well as quantification approaches (the external calibration for WDXRF and the internal standard for TXRF) were applied according to the features of the analyzed samples. The rock-forming oxides ($Na_2O$, MgO, $Al_2O_3$, $SiO_2$, $P_2O_5$, $K_2O$, CaO, $TiO_2$, MnO, and $Fe_2O_3$) and trace elements (V, Cr, Ni, Cu, Zn, Rb, Sr, Y, Ba, and Pb) were quantified in soils, as well as several elements (Na, Mg, Al, Si, P, S, Cl, K, Ca, Ti, Cr, Mn, Fe, Ni, Cu, Zn, Br, Rb, Sr, Pb, and Ba) were quantified in pine needles. Comparing the results of soils and pine needles analysis with the regional background values indicated a significant contamination pollution level of the studied area.

**Keywords:** aluminum industry; soil; pine needle; wavelength-dispersive X-ray fluorescence; total reflection X-ray fluorescence; pollution; geochemical indices

**Citation:** Chubarov, V.; Cherkashina, T.; Maltsev, A.; Chuparina, E.; Amosova, A.; Prosekin, S. Investigation of Soils and Pine Needles Using WDXRF and TXRF Techniques for Assessment of the Environmental Pollution of Shelekhov District, Eastern Siberia, by the Aluminum Industry and Heat Power Engineering. *Agronomy* **2022**, *12*, 454. https://doi.org/10.3390/agronomy12020454

Academic Editors: Roberto Terzano, Ignazio Allegretta, Fabjola Bilo, Eva Marguí and Galina V. Pashkova

Received: 18 December 2021
Accepted: 10 February 2022
Published: 11 February 2022



## 1. Introduction

X-ray fluorescence (XRF) spectrometry is widely used for the analysis of several kinds of samples, including rocks, soils, plants, industrial wastes, etc. [1,2] XRF is actually applied for the environmental monitoring of urbanized areas, potentially polluted by the industrial emissions. Investigation of pollution indicators in some samples (such as soils and pine needles), represents a complementary tool for environmental monitoring and studying of different types of anthropogenic contributions, e.g., industrial and traffic emissions [3–11]. XRF methods enable fast multi-elemental analysis of soils using portable energy dispersive (EDXRF) equipment [12–17] and quantitative analysis using benchtop wavelength dispersive (WDXRF) equipment [1,18–24]. Several XRF techniques were also developed for pine needles analysis [25–30]. However, features of the samples and applied equipment require specific approaches for sample preparation strategies and quantification procedures.

The WDXRF method is a common technique for the determination of major elements in geological objects. This method primarily uses two sample preparation techniques:

pressing of powder to a pellet [31] and fusion of powder with flux to obtain a homogeneous glass disk [32]. Fusion is a versatile technique for WDXRF analysis of soils due to its ability to minimize the effects of particle size and mineralogical composition. Additionally, the certified reference materials (CRMs) of different types of rocks can be used to construct calibration curves, and the best accuracy can be achieved in the determination of major and minor elements. The disadvantages of this technique are its relatively high limits of detection (LOD) for minor and trace elements due to the dilution of the sample by flux, as well as the losses of some important volatile elements (As, Br, S) during the fusion. Unlike soils, the bulk of the raw plants is water (85–90%). The dry plant matter mainly consists of carbon, nitrogen, oxygen, and hydrogen (up to 99%), the organic matter is represented mainly by cellulose, and the total content of the rest inorganic components may not exceed 0.1%. Hence, the optimal sample preparation technique for plants is pressing powder as a pellet.

Total-reflection X-ray fluorescence (TXRF) spectrometry is a particular XRF method in which the primary beam hits the sample at an angle lower than 0.1° in order to obtain the reflection of the whole beam on the reflector [33,34]. The reflection of most of the incident beam radiation reduces the spectral background and minimizes absorption effects, which allows better LOD values compared to those of conventional energy-dispersive spectrometers. TXRF was applied for the multi-elemental [35–41], as well as single-element (Br[42], Se[43] and As[44]) analysis of soils. TXRF analysis was also applied to different plant samples [45–50], including pine needles [49,50].

In this work, WDXRF and TXRF were used to analyze soils and pine needles from areas potentially contaminated by the aluminum industry emissions. The following elements were chosen as potential pollutants: As, Pb, Zn, Co, Ni, Cu, Cr, Ba, V, W, Mn, and Sr. Aluminum was also analyzed due to the specificity of the industrial site. Most of the above mentioned elements are also toxic for plants. Determination of other elements, such as Na, Mg, Si, P, K, Ca, Ti, and Fe is necessary to characterize investigated samples. This article discusses the development of the TXRF and WDXRF techniques for the complex study of compositions of pine needles and soils as indicators of industrial pollution. Environmental studies were already led on the investigated area [26,51–58] however, in this work a strategy based on X-ray methods has been developed.

## 2. Materials and Methods

### *2.1. Field Description, Sampling, and Preliminary Preparation*

A total of 14 soil and 13 pine needle samples were collected from the area located near Irkutsk aluminum smelter (IrkAZ), Shelekhov, Irkutsk region, Russia. The IrkAZ is one of the largest smelters in Russia and it is the oldest in Eastern Siberia. Some facilities, such as JSC "Kremnii" (silicon production), JSC "Irkutskkabel'" (cable production), and combined heat and power plant (CHP) are in the facility territory. The sampling scheme was drawn up considering the wind rose. The location of industrial enterprises and features of the terrain were estimated using a global digital elevation model of Shuttle Radar Topography Mission [59]. On the right bank of the Irkut River, the terrain is limited by the Olkhinskoe plateau, therefore the altitude of the right bank exceeds the altitude of the industrial area of the IrkAZ with the maximum height of the pipes of 80 m. Therefore, most of the emissions settle near the left bank of the Irkut River, and the studied area has an oval shape (Figure 1).

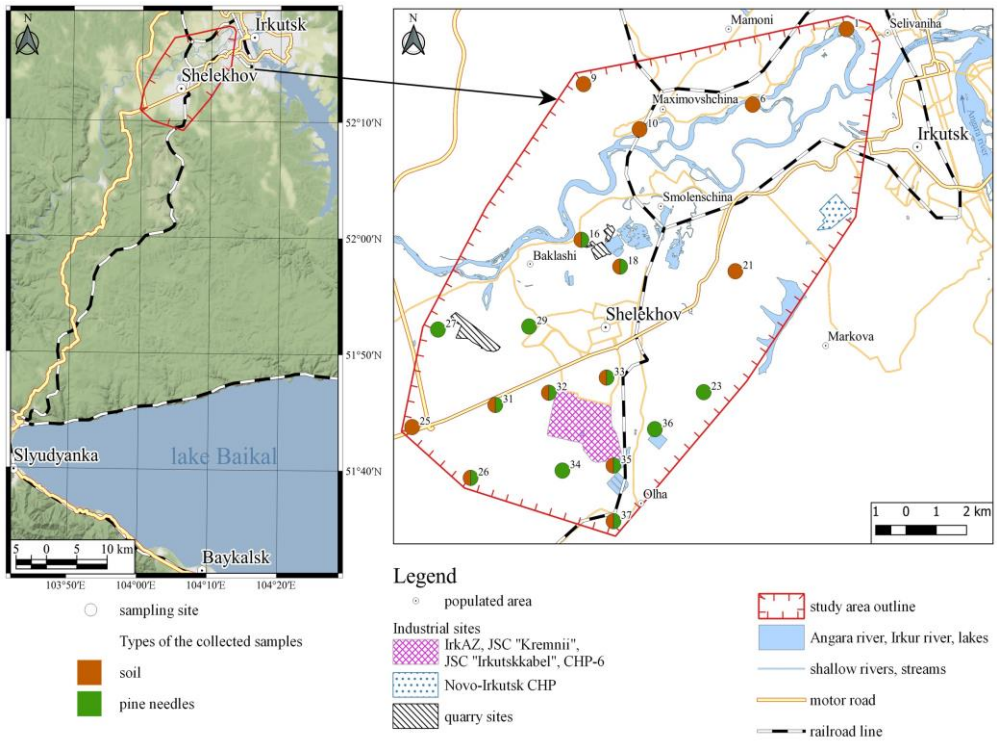


**Figure 1.** Map and scheme of the studied area.

*Pine needles sampling.* Pine needle samples (13 pieces) were collected from five model trees at the end of the growing season in August of 2018. A feature of pine needles in comparison with other types of terrestrial plants is the presence of resinous organic substances, which complicates the routine grinding procedure of air-dried green needles to a fine powder. The application of an electric grinder led simultaneously to the presence of both fine dust-like particles and big fragments of needles 1–2 mm in length. In addition, the material is highly electrified. Therefore, pine needle samples were preliminarily dried at a temperature of 80 °C for 24 h, then they were ground in an electric grinder. Finally, they were manually milled to particle size less than 75 μm using an agate mortar.

*Soil sampling.* Soil samples (14 pieces) were collected from the first 15 cm of the surface horizon where heavy metals have accumulated [60,61] showing an ecological imbalance in the environment. Inclusions, such as stones, roots, glass, were removed. After that, samples were air dried at an ambient temperature for 24 h, and then they were additionally dried at 110 °C until they reached a constant weight. Finally, samples were sieved and milled to a particle size less than 75 μm.

For further analysis, all collected soil and pine needle samples were prepared in accordance with the document [62].

## 2.2. Reference Materials

The quality assurance control of the WDXRF and TXRF results, as well as the construction of calibration curves for WDXRF, were carried out using the CRMs of different types of igneous, sedimentary rocks, soils, and plants. The following CRMs were used for soil samples analysis: AGV-2, BHVO-2, RGM-1, and DTS-1 (the United States Geological Survey [63]), GSS-6 (the Institute of Geophysical and Geochemical Exploration, Langfang, China [64]), SDU-1, ST-2, SNS-2, SSN-1, SG-3, SG-4, SKD-1, GBPG-1, SGD-2, SGHM-1, SA-1, and SSV-1 (Vinogradov Institute of Geochemistry, Siberian Branch of the Russian Academy of Sciences, Irkutsk, Russia [65]), SDO-1, SDO-2, SDO-8, SDO-9, SP-1, and SP-3 (the Institute of Applied Physics, Irkutsk State University, Irkutsk, Russia [66,67]). The following CRMs were used for pine needles analysis: LB-1 (leaf of birch), Tr-1 (mixture of

meadow herbs), and HSS-1 (pine needles) provided by Vinogradov Institute of Geochemistry, Siberian Branch of the Russian Academy of Sciences (Irkutsk, Russia) [65,68], INCT-SBF-4 (soya bean flour) and INCT-MPH-2 (mixed polish herbs) provided by the Institute of Nuclear Chemistry and Technology (Warsaw, Poland) [69,70], SBMK-02 (potatoes tuber) and SBMP-02 (wheat grain) provided by the Siberian Research Institute of Soil Management and Chemicalization of Agriculture, Siberian Branch of the Russian Academy of Agricultural Sciences (Krasnoobsk, Russia) [71], and GSV-4 (tea leaves) provided by the Institute of Geophysical and Geochemical exploration (Langfang, China) [72]. The chemical composition and origin data for the CRMs were taken from the compilation [73] and GeoReM database [74].

### *2.3. WDXRF*

#### 2.3.1. Instrumentation

All measurements were performed using a WDXRF-spectrometer S4 Pioneer (Bruker AXS, Karlsruhe, Germany). This instrument is equipped with a 4 kW power X-ray tube with an Rh-anode, Be window of 75 μm thickness, a gas flow proportional (GFPC) counter for light element detection, and a scintillation counter (SC) for heavy elements. The X-ray spectra, numerical peak separation, and correction of the matrix effects were processed by the spectrometer software [75]. Table 1 presents the instrumental operation conditions for WDXRF analysis of pine needle and soil samples.

**Table 1.** WDXRF instrumental measurement conditions for soil and pine needle samples.

| Analytical Line | kV/mA | Crystal/Detector | Counting Time, s |
|---|---|---|---|
| Soils (prepared as fused beads) | | | |
| $NaK_{\alpha 1,2}$ | 30/80 | OVO-55/GFPC | 60 |
| $MgK_{\alpha 1,2}$ | 30/80 | OVO-55/GFPC | 30 |
| $AlK_{\alpha 1,2}$ | 30/80 | PET/GFPC | 30 |
| $SiK_{\alpha 1,2}$ | 30/80 | PET/GFPC | 15 |
| $PK_{\alpha 1,2}$ | 30/80 | PET/GFPC | 60 |
| $KK_{\alpha 1,2}$ | 30/80 | LiF200/GFPC | 30 |
| $CaK_{\alpha 1,2}$ | 30/80 | LiF200/GFPC | 30 |
| $TiK_{\alpha 1,2}$ | 30/80 | LiF200/GFPC | 30 |
| $MnK_{\alpha 1,2}$ | 50/40 | LiF200/GFPC | 30 |
| $FeK_{\alpha 1,2}$ | 50/40 | LiF200/SC | 15 |
| Pine needles (prepared as pressed pellets) | | | |
| $NaK\alpha_{1,2}$ | 30/60 | OVO-55/GFPC | 30 |
| $MgK\alpha_{1,2}$ | 30/60 | OVO-55/GFPC | 10 |
| $PK_{\alpha 1,2}$ | 30/60 | PET/GFPC | 10 |
| $KK_{\alpha 1,2}$ | 30/60 | PET/GFPC | 10 |
| $SK_{\alpha 1,2}$ | 30/60 | PET/GFPC | 10 |
| $ClK_{\alpha 1,2}$ | 30/50 | PET/GFPC | 30 |
| $CaK_{\alpha 1,2}$ | 40/50 | LiF200/GFPC | 10 |
| $TiK_{\alpha 1,2}$ | 40/50 | LiF200/GFPC | 20 |
| $MnK_{\alpha 1,2}$ | 50/40 | LiF200/SC | 20 |
| $FeK_{\alpha 1,2}$ | 50/40 | LiF200/SC | 10 |
| $ZnK_{\alpha 1,2}$ | 50/40 | LiF200/SC | 20 |
| $BrK_{\alpha 1,2}$ | 50/40 | LiF200/SC | 30 |
| $BaL_{\alpha 1,2}$ | 40/50 | LiF200/GFPC | 30 |

Analysis was made in vacuum mode to avoid signal losses by air absorption. Optimal background positions for analytical lines were chosen under the following rules. The background position must be free from the occurrence of intense lines of other elements

presented in the sample. The relation between background intensities for each analytical line and the background intensities for the chosen angular positions must not depend on variations in the chemical composition of the samples examined. The quantification model was designed using certified reference material for calibration.

2.3.2. Sample Preparation Approaches

*Pine needles.* All chosen CRMs of plants and pine needle samples were prepared as pressed pellets on the boric acid substrate. The mass of 0.500 ± 0.001 g of the ground sample was evenly distributed on the 38 mm diameter press form surface. The boric acid powder was added as a bottom pellet layer and the specimen was pressed into a pellet with a 14 ton force. Pellets were kept in a desiccator before measuring.

*Soils.* To prepare fused beads, all the samples were preliminarily dried at 110 °C to remove moisture and then calcined in the muffle furnace for 4 hours at a temperature of 950 °C, and loss of ignition values was calculated. A mixture of lithium metaborate and lithium tetraborate was preliminarily dried at 450 °C for 4 hours. The mass of 0.500 ± 0.001 g of the calcined sample was mixed with 7.5 ± 0.001 g of borates mixture ($Li_2B_4O_7/LiBO_2$, 65/35, Claisse, Québec, QC, Canada). The dilution factor was 16. Afterward, 7 drops of 40 mg/ml of the LiBr solution were added as a releasing agent. The obtained mixture was fused in the platinum crucible in the automatic electric furnace TheOX (Claisse, Québec, QC, Canada) for 19 minutes at a temperature of 1050 °C [76].

2.3.3. Quantitative Analysis

To obtain elements concentrations, calibration curves (as the dependence on elements concentration on the intensity of analytical line) were constructed. For soils analysis the fundamental parameters method for matrix effects correction (the "variable alphas" option) was used:

$$C_i^* = C_i \cdot (1 + \sum_{j \neq i}^{n} a_{ij} \cdot C_j), \quad (1)$$

where $C_i^*$ is the corrected concentration of the analyzed element, $C_j$ is the concentration of the matrix element, $\alpha_{ij}$ is the matrix correction coefficient.

For pine needles analysis the empirical influence coefficients for matrix effects correction were applied:

$$C_i^* = C_i \cdot (1 + \sum_{j \neq i}^{n} a_{ij} \cdot I_j), \quad (2)$$

where $I_j$ is the intensity of the influencing element.

Statistical processing of WDXRF (and further TXRF) results was performed by the recommendations given at a 95% confidence interval [77,78]. The LOD values were assessed according to the 3σ approach:

$$LOD = 3 \times \sigma_b \times \left(C^{cert} / I_{net}\right), \quad (3)$$

where $\sigma_b$ is the square root of the background intensity (count rate), $I_{net}$ is the net intensity (count rate), $C^{cert}$ is the certified value of element concentration in the CRM. The limit of quantification (LOQ) values were accessed according to the 10σ approach and were approximately 3.3 times greater than the LOD values.

*2.4. TXRF*

2.4.1. Instrumentation

TXRF analysis was performed using a benchtop spectrometer S2 PICOFOX (Bruker Nano, Germany) equipped with a Mo-anode X-ray tube (working conditions are 50 kV

and 0.75 mA), multilayer monochromator, and silicon drift detector (the effective area is 30 $mm^2$) with an energy resolution <150 eV at MnKα line. All measurements were carried out during 500 s. Siliconized quartz carriers were used as sample holders and reflectors. Spectra processing and quantitative analysis were carried out using the spectrometer software SPECTRA 7.8.2 [79].

#### 2.4.2. Sample Preparation Approaches

*Pine needles.* The mass of 50 mg of milled pine needle sample, 1500 μL of concentrated nitric acid (supra-pure grade, Merck, Darmstadt, Germany), and 100 μL of hydrogen peroxide was put in a vessel, closed, and heated carefully. Then, 100 μL of the internal standard of Ga (100 mg/L) was put into a vessel and brought to a volume of 5000 μL by ultrapure deionized water (18.2 MW, Elga Labwater, High Wycombe, UK). A volume of 5 μL of the obtained solution was deposited onto the carrier and dried on a heating plate.

*Soils.* The mass of 20 mg of milled soil sample was placed in a plastic tube, and 2 mL of aqueous 1% Triton X-100 solution (Merck, Darmstadt, Germany) and 100 μL of the internal standard (Ga) were added. The suspension was mixed thoroughly using a Vortex shaker (IKA, Staufen im Breisgau, Germany). A volume of 5 μL of this suspension was deposited onto the carrier and dried on a heating plate.

#### 2.4.3. Quantitative Analysis

The concentration value $C_i$ of the element (in μg/g) was calculated by the following equation:

$$C_i = \frac{C_{is} \times I_i \times S_{is}}{I_{is} \times S_i}, \quad (4)$$

where $C_{is}$ is the concentration of the internal standard; $I_i$, $I_{is}$ are the net peak area of an element of interest and the internal standard, respectively; $S_i$, $S_{is}$ are the sensitivities of an element of interest and the internal standard, respectively. Sensitivities $S_i$, $S_{is}$ are embedded in the SPECTRA software of the instrument and relevant for all the samples satisfied the thin layer conditions.

### *2.5. Data Processing*

There are dozens of works devoted to assessing the soil pollution level in different industrial areas in the world by heavy metals [7,80–82]. In this study, four geochemical indices, including the contamination factor ($C_f$), normalized enrichment factor (EF), pollution load index (PLI), and geoaccumulation index ($I_{geo}$) were applied to assess the potential soil contamination level by toxic elements (As, Pb, V, Cr, Ni, Cu, Zn, Sr, Mn) and their possible sources [21]. Such information is very important for the preservation of the environment and human health because these toxic elements belong to Groups 1–3 of toxic chemicals according to World Health Organization classifications, IARC [22,83].

The $C_f$ factor is used to assess the potential ecological risk of pollutants in soils [84,85]. With this approach, $C_f$ accounts for the pollution of a single element according to the concentration background. It was defined as the ratio of the heavy metal average concentrations ($C^i$) in the top horizon (depth ~ 15 cm) to the regional background values ($C_b^i$) [52,86,87]:

$$C_f = C^i / C_b^i. \quad (5)$$

In accordance with [86], $C_f$ is categorized into the following classes: $C_f < 1$ (low contamination level), $1 \le C_f < 3$ (moderate contamination level), $3 \le C_f < 6$ (considerable contamination level), $6 \le C_f$ (very high contamination level).

The level of contamination and possible sources of these toxic metals are effectively assessed using the EF method. The EF is a normalization method proposed by Simex and

Helz [88] to evaluate metal concentration. For our purpose, Fe was chosen as the most appropriate soil constituent for normalization because the constituent should be associated with finer particles. Moreover, Fe was applied to reduce the metal variability caused by grain size and mineralogy in this study. The EF for each metal is defined as follows [89]:

$$EF = \frac{(C_i / C_{Fe})}{(C_i / C_{Fe})_b}, \quad (6)$$

where $(C_i/C_{Fe})$ is the ratio of metal and Fe concentrations in the soil sample, and $(C_i/C_{Fe})_b$ is the ratio of metal and Fe concentrations of the regional background. According to Sutherland [81], the EF factor is used to classify the soils into five categories: EF < 2 (deficiency to minimal enrichment), 2 < EF < 5 (moderate enrichment), 5 < EF < 20 (significant enrichment), 20 < EF < 40 (very high enrichment), EF > 40 (extremely high enrichment). However, in agreement with Zhang and Liu [90], the values of 0.5 ≤ EF ≤ 1.5 denote that the enrichment of trace metals is basically of crustal origin, whereas an EF > 1.5 suggests that the source of the metals is more anthropogenic.

The PLI method was proposed by Tomlinson [91] to assess the overall level of heavy metal pollution. The PLI index was computed from the following expression:

$$PLI = \left(C_{f1} \times C_{f2} \times C_{f3} \times \ldots \times C_{fn}\right)^{1/n}, \quad (7)$$

where $C_f$ is the contamination index of toxic metals assessed above, and $n$ is the number of species involved in the assessment of toxic metals. This method is convenient for assessing the pollution load for individualized sites by expressing the concentrations of all individual elements under consideration. The pollution levels were divided into four grades according to [92]: PLI < 1 (no pollution), 1 < PLI < 2 (moderate pollution), 2 < PLI < 3 (heavy pollution), and 3 < PLI (extremely heavy pollution).

The $I_{geo}$ index was introduced by Muller [93] to define heavy metal pollution in soils by comparing current concentrations with preindustrial levels. In addition to the EF method, this approach not only defines possible sources of the metal examined but also takes into account the natural concentrations fluctuations of a substance, as well as small anthropogenic influences [94]. The $I_{geo}$ index is expressed as follows:

$$I_{geo} = \log_2\left(C_i / 1.5C_{i,b}\right), \quad (8)$$

where $C_i$ is the measured concentration of element in the soil sample, $C_{i,b}$ is the regional background value of element $n$ in the study area, and the constant 1.5 allows analysis of the natural concentrations fluctuations of a substance in the environment and detection of small anthropogenic influences. Seven classes based on the $I_{geo}$ index were recognized [80]: $I_{geo} \leq 0$ (practically uncontaminated), $0 < I_{geo} < 1$ (uncontaminated to moderately contaminated), $1 < I_{geo} < 2$ (moderately contaminated), $2 < I_{geo} < 3$ (moderately to heavily contaminated), $3 < I_{geo} < 4$ (heavily contaminated), $4 < I_{geo} < 5$ (heavily to extremely contaminated), $5 < I_{geo}$ (extremely contaminated).

Presentation of the data was performed using STATISTICA 10 software.

## 3. Results and Discussion

### *3.1. XRF Spectra and Quantitative Analysis*

#### 3.1.1. WDXRF and TXRF Spectra

Figure 2 presents the WDXRF spectra of the CRMs GSS-6 (soil) and HSS-1 (pine needles) registered in the 0-24 keV energy range.

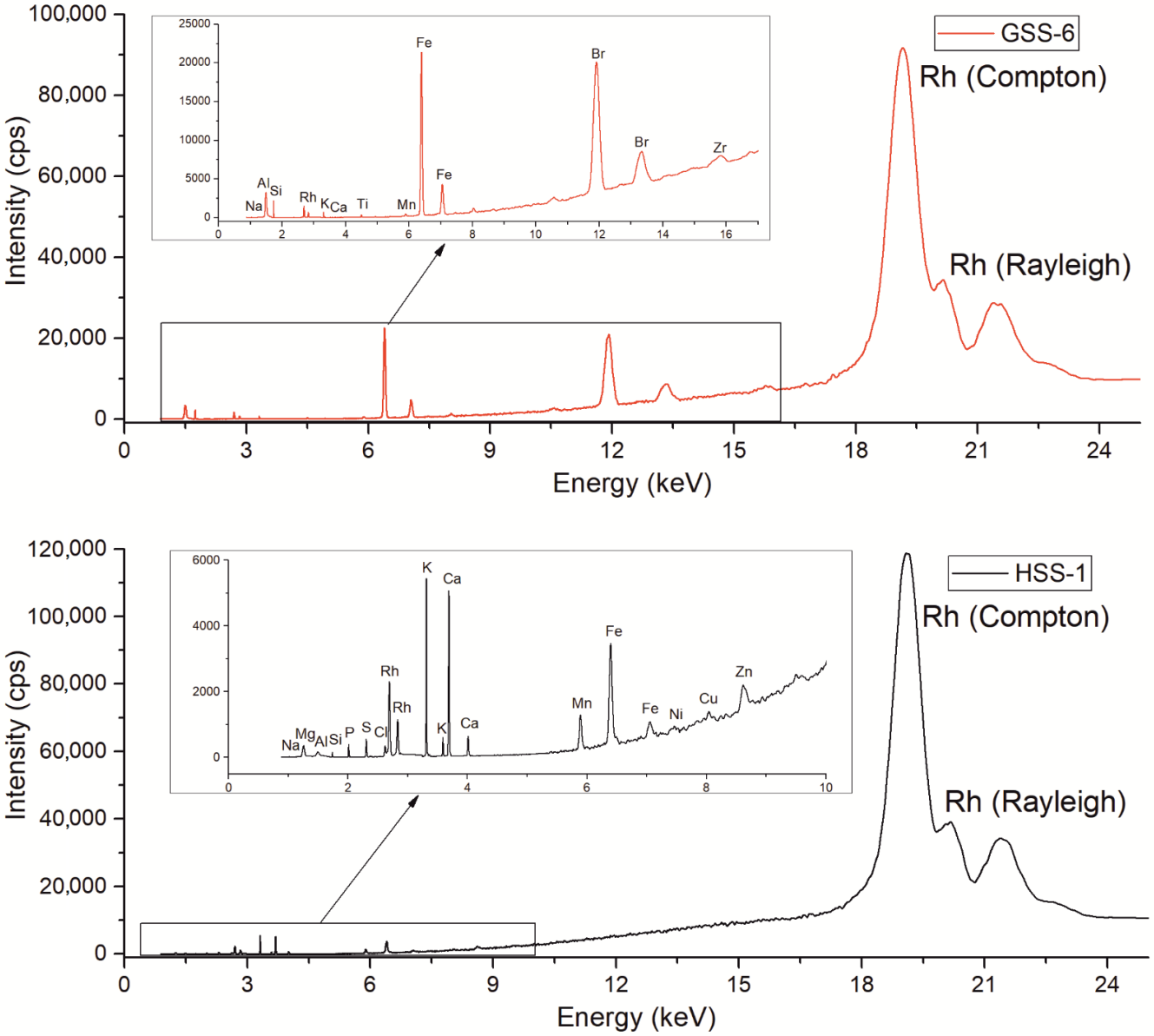


**Figure 2.** WDXRF spectra of the CRM of soil GSS-6 prepared as glass disk (red line) and the CRM of pine needles HSS-1 prepared as a pressed pellet (black line)

The peaks of Br derived from the use of the LiBr additions for preparing the glass disk. Tiny peaks of Cu and Zn in the spectra present the equipment background, peaks of Rh – Compton–Rayleigh scattering radiation.

Figure 3 presents the TXRF spectra of soil and pine needle samples in 0-20 keV energy range.

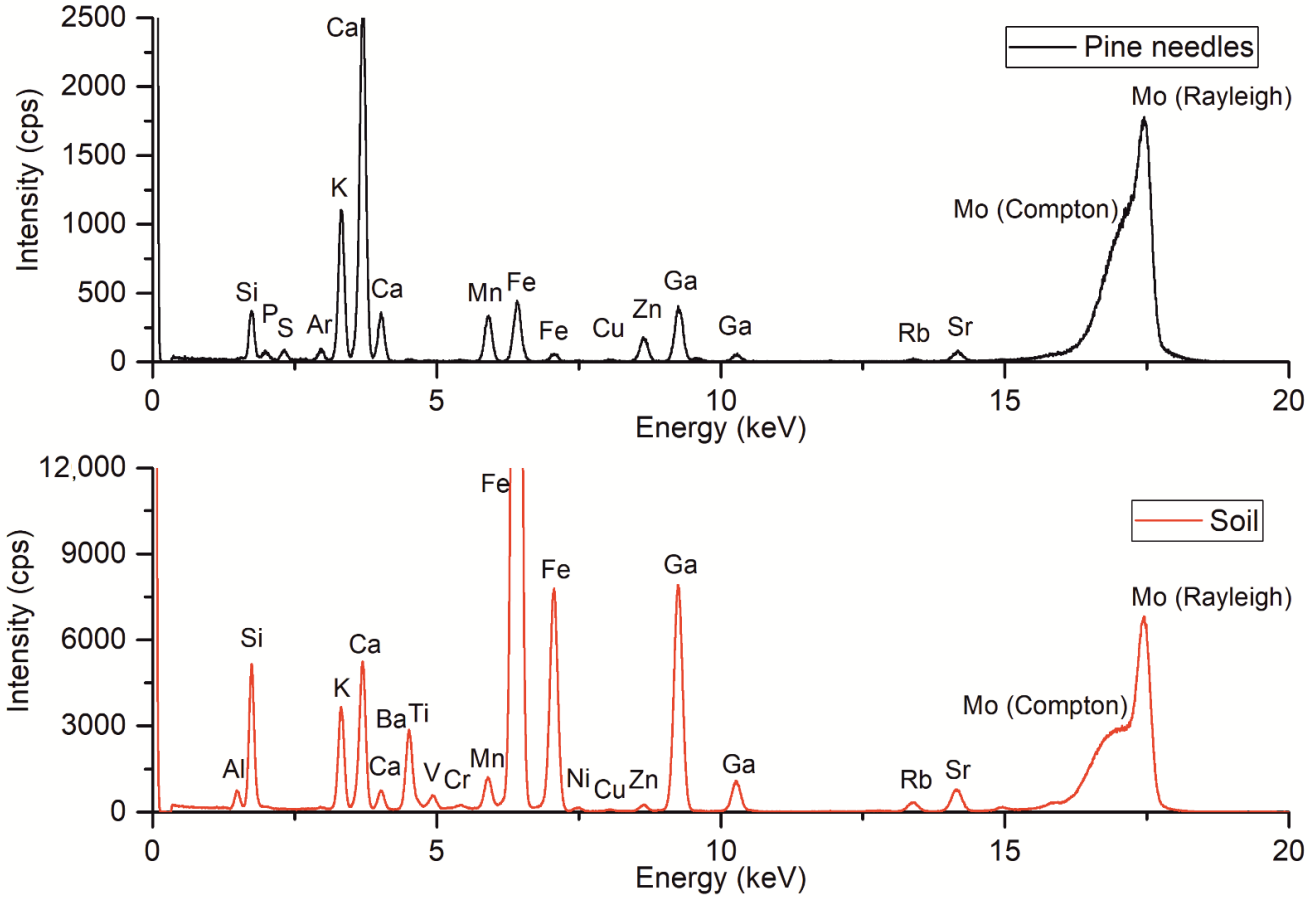


**Figure 3.** TXRF typical spectra of pine needle (black line) and soil (red line) samples

The peaks of Si partially derived from the use of the quartz carrier as a sample holder. Tiny peaks of Ar in both spectra demonstrate the air impact in the instrumental system, peaks of Mo—Compton-Rayleigh scattering radiation; peaks of Ga—the usage of the internal standard. Other elements in the spectra present the elemental composition of samples analyzed by TXRF. The LOD values for the determination of trace elements in soils are in the range of 1.0-10 μg/g, except for Ba (LOD=30 μg/g); for pine needles the LOD values are in the range of 0.2 – 1.1 μg/g, except for Ba (LOD=6.0 μg/g). Detailed data are presented in the Supplementary materials, Table S3.

### 3.1.2. Quantitative WDXRF Analysis and Statistical Processing

*Quantitative WDXRF analysis and statistical processing for soils.* To construct calibration curves, 20 CRMs of igneous and sedimentary rocks were used (see section 2.2). Table 2 presents the calibration ranges and statistical data obtained, including LOD and root mean square (RMS) values examined characterizing dispersion point around the calibration line. All the rock-forming elements were expressed as oxides.

**Table 2.** Statistical data obtained for WDXRF analysis of major oxides in soil samples.

| Oxide | Calibration range, wt% | RMS, wt% | LOD, wt% |
|---|---|---|---|
| $Na_2O$ | 0.035–9.96 | 0.1 | 0.02 |
| MgO | 0.079–49.59 | 0.2 | 0.02 |
| $Al_2O_3$ | 0.19–31.89 | 0.3 | 0.01 |
| $SiO_2$ | 39.58–73.80 | 0.7 | 0.04 |
| $P_2O_5$ | 0.01–1.03 | 0.02 | 0.01 |
| $K_2O$ | 0.01–18.0 | 0.02 | 0.006 |

| | | | |
|---|---|---|---|
| CaO | 0.17–11.40 | 0.3 | 0.002 |
| $TiO_2$ | 0.018–2.73 | 0.03 | 0.009 |
| MnO | 0.009–1.77 | 0.01 | 0.003 |
| $Fe_2O_3$ | 0.94–12.30 | 0.2 | 0.005 |

*Quantitative WDXRF analysis and statistical processing for pine needles.* To construct calibration curves, seven CRMs of plants were used (see section 2.2). Table 3 presents the calibration ranges and statistical data obtained, including RMS and LOD values.

**Table 3.** Statistical data obtained for WDXRF analysis of major and trace elements in pine needle samples.

| Element | Calibration range, μg/g | RMS, μg/g | LOD, μg/g |
|---|---|---|---|
| Na | 44–750 | 80 | 30 |
| Mg | 950–4400 | 170 | 20 |
| Al | 20–3000 | 40 | 10 |
| Si | 65–5500 | 90 | 20 |
| P | 1050–6500 | 310 | 20 |
| K | 4200–24200 | 1200 | 10 |
| Ca | 540–16000 | 700 | 20 |
| Ti | 3–59 | 3 | 3 |
| Mn | 7–1240 | 8.8 | 2 |
| Fe | 54–970 | 7 | 10 |
| S | 1000–4200 | 170 | 10 |
| Cl | 450–3600 | 170 | 100 |
| Zn | 23–93.7 | 4.8 | 3 |
| Br | 2.4–9.0 | 3.7 | 2 |
| Ba | 7–230 | 7.8 | 5 |

3.1.3. Validation of the Methods

The accuracy of the WDXRF and TXRF results was validated by measuring the CRMs of soils (SP-1, SP-3, and GSS-6) and plants (INCT-MPH-2, HSS-1) As and Br were not quantified in the CRMs INCT-MPH-2 and HSS-1 by TXRF due to losses during the acid digestion procedure. To assess the deviation between the measured and certified concentration values for the elements determined, the recovery $R_i$ was computed as:

$$R_i = \frac{C_i}{C^{cert}} \cdot 100\%, \quad (9)$$

where $C^{cert}$ is the certified concentration of an element in the CRM, $C_i$ is the measured concentration of element $i$ in the CRM. The obtained $R_i$ values are shown in Tables 4, 5, and 6.

**Table 4.** The WDXRF results validation with the CRMs of soils.

| Oxide | SP-1 | | | SP-3 | | | GSS-6 | | |
|---|---|---|---|---|---|---|---|---|---|
| | $C^{cert}$, wt% | $C^{WDXRF}$, wt% | $R_i$, % | $C^{cert}$, wt% | $C^{WDXRF}$, wt% | $R_i$, % | $C^{cert}$, wt% | $C^{WDXRF}$, wt% | $R_i$, % |
| $Na_2O$ | 0.80±0.03 | 0.8±0.1 | 100 | 1.16±0.05 | 1.2±0.1 | 103 | 0.19±0.02 | 0.2±0.1 | 105 |
| MgO | 1.02±0.03 | 1.0±0.1 | 98 | 1.95±0.04 | 2.0±0.1 | 103 | 0.34±0.05 | 0.4±0.1 | 118 |
| $Al_2O_3$ | 10.37±0.08 | 10.5±0.3 | 101 | 12.61±0.07 | 12.5±0.3 | 99 | 21.23±0.16 | 21.1±0.3 | 99 |
| $SiO_2$ | 69.73±0.21 | 70.8±0.9 | 102 | 65.72±0.08 | 65.9±0.9 | 100 | 56.93±0.18 | 57.1±0.8 | 100 |
| $P_2O_5$ | 0.17±0.01 | 0.16±0.01 | 94 | 0.21±0.01 | 0.21±0.01 | 100 | 0.069±0.007 | 0.07±0.01 | 101 |

| | | | | | | | | | |
|---|---|---|---|---|---|---|---|---|---|
| $K_2O$ | 2.29±0.06 | 2.33±0.02 | 102 | 2.51±0.13 | 2.63±0.02 | 105 | 1.70±0.06 | 1.70±0.03 | 100 |
| CaO | 1.63±0.05 | 1.6±0.1 | 98 | 2.86±0.06 | 2.8±0.1 | 98 | 0.22±0.03 | 0.2±0.1 | 91 |
| $TiO_2$ | 0.75±0.02 | 0.77±0.03 | 103 | 0.73±0.01 | 0.76±0.03 | 104 | 0.73±0.02 | 0.74±0.03 | 101 |
| MnO | 0.077±0.002 | 0.08±0.01 | 104 | 0.092±0.002 | 0.09±0.01 | 98 | 0.19±0.01 | 0.19±0.01 | 100 |
| $Fe_2O_3$ | 3.81±0.05 | 4.0±0.1 | 105 | 4.91±0.04 | 5.1±0.1 | 104 | 8.09±0.13 | 8.1±0.2 | 100 |

**Table 5.** The WDXRF results validation with the CRMs of plants.

| | INCT-MPH-2 | | | HSS-1 | | |
|---|---|---|---|---|---|---|
| Element | $C^{cert}$, μg/g | $C^{WDXRF}$, μg/g | $R_i$, % | $C^{cert}$, μg/g | $C^{WDXRF}$, μg/g | $R_i$, % |
| Na | *350* [a] | 336±42 | 96 | 44±4 | 42±14 | 95 |
| Mg | 2920±180 | 2970±380 | 102 | 1200±200 | 1220±60 | 102 |
| Al | 670±111 | 570±70 | 85 | 190±30 | 197±3 | 104 |
| Si | n/cert [b] | 4330±210 | n/calc [c] | 1100±400 | 1110±300 | 101 |
| P | *2500* | 2920±180 | 117 | 1400±200 | 1470±110 | 105 |
| K | 19100±1200 | 18800±400 | 98 | 4600±300 | 4820±90 | 105 |
| Ca | 10800±700 | 11300±200 | 104 | 4200±200 | 4700±300 | 112 |
| Ti | *34* | 47±10 | 138 | 11±3 | 13±4 | 118 |
| Mn | 191±12 | 179±7 | 94 | 215±12 | 243±24 | 113 |
| Fe | *460* | 476±40 | 103 | 470±60 | 570±70 | 121 |
| S | 2410±140 | 2190±170 | 91 | 1020±100 | 910±100 | 112 |
| Cl | 2840±200 | 2710±173 | 95 | *370* | n/d [d] | n/calc |
| Br | 7.7±0.6 | 5.2±2.8 | 67 | *1.2* | n/d | n/calc |
| Ba | 32.5±2.5 | 39.0±6.2 | 120 | 4.8±0.4 | 5.5±2.0 | 115 |

[a] Approximate value of element concentration; [b] this concentration is not certified; [c] this value cannot be calculated; [d] this concentration is not detected as the WDXRF result is lower than the limit of detection (LOD) value.

Agreement between the results certified and obtained by WDXRF was found to be satisfactory and within the interval of 94–105% for soils (excluding overestimation for MgO (118 %) and underestimation for CaO (91%) in CRM GSS-6) and within the interval of 85–121% for pine needles (the comparison with the approximate values was excluded). Significant discrepancies in the recovery values were observed for Ba, Br, and Ti due to the high values of total uncertainty for low element concentrations in these plant CRMs.

**Table 6.** The TXRF results validation with the CRMs of soils and plants.

| | SP-1 | | | SP-3 | | | GSS-6 | | | INCT-MPH-2 | | | HSS-1 | | |
|---|---|---|---|---|---|---|---|---|---|---|---|---|---|---|---|
| | $C^{cert}$, μg/g | $C^{TXRF}$, μg/g | $R_i$, % | $C^{cert}$, μg/g | $C^{TXRF}$, μg/g | $R_i$, % | $C^{cert}$, μg/g | $C^{TXRF}$, μg/g | $R_i$, % | $C^{cert}$, μg/g | $C^{TXRF}$, μg/g | $R_i$, % | $C^{cert}$, μg/g | $C^{TXRF}$, μg/g | $R_i$, % |
| V | 77 ± 8 | 51 ± 15 | 68 | 110 ± 10 | 88 ± 7.0 | 80 | 130 ± 7 | 51 ± 6.7 | 39 | 0.95 ± 0.16 | n/d [a] | n/calc [b] | 0.27 ± 0.04 | n/d | n/calc |
| Cr | 82 ± 5 | 115 ± 19 | 140 | 140 ± 10 | 165 ± 83 | 118 | 75 ± 6 | 116 ± 3 | 154 | 1.70 ± 0.13 | n/d | n/calc | 3.6 ± 0.3 | n/d | n/calc |
| Mn | 596 ± 15 | 624 ± 32 | 105 | 705 ± 15 | 699 ± 28 | 99 | 1470 ± 82 | 1820 ± 56 | 124 | 191 ± 12 | 161 ± 5 | 84 | 215 ± 12 | 267 ± 11 | 124 |
| Ni | 33 ± 3 | 30 ± 2 | 91 | 56 ± 4 | 49 ± 5 | 88 | 53 ± 4 | 51 ± 1 | 96 | 1.60 ± 0.16 | 1.1 ± 0.2 | 70 | 2.0 ± 0.1 | 1.5 ± 0.1 | 75 |
| Cu | 22 ± 1 | 27 ± 3 | 123 | 30 ± 1 | 30 ± 3 | 100 | 390 ± 14 | 445.0 ± 0.1 | 114 | 7.80 ± 0.53 | 8.1 ± 0.7 | 104 | 3.8 ± 0.2 | 3.8 ± 0.3 | 100 |
| Zn | 52 ± 2 | 67 ± 5 | 129 | 73 ± 2 | 82 ± 6 | 112 | 97 ± 6 | 115 ± 3 | 118 | 33.0 ± 2.1 | 29 ± 1 | 87 | 45 ± 3 | 55 ± 0.9 | 124 |
| As | n/cert [c] | 7 ± 2 | n/calc | n/cert | 9 ± 1 | n/calc | 220 ± 14 | 250 ± 10 | 114 | n/cert | n/d | n/calc | (0.2 | n/d | n/calc |
| Br | n/cert | 12 ± 3 | n/calc | n/cert | 14 ± 4 | n/calc | 8.0 ± 0.7 | 8.6 ± 0.4 | 108 | 7.7 ± 0.6 | n/d | n/calc | (1.2) | n/d | n/calc |
| Rb | 84±15 | 103 ± 13 | 123 | 85 ± 5 | 90 ± 7 | 106 | 237 ± 8 | 263 ± 5 | 111 | 11.0 ± 0.7 | 10 ± 1 | 94 | 2.3 ± 0.2 | 2.3 ± 0.1 | 99 |
| Sr | 130±20 | 107 ± 9 | 82 | 160 ± 3 | 120 ± 4 | 75 | 39 ± 4 | 46 ± 2 | 119 | 38.0 ± 2.7 | 38 ± 2 | 100 | 11 ± 1 | 15 ± 0.04 | 136 |
| Y | *39* [a] | 35 ± 22 | 90 | 28 ± 2 | 26 ± 10 | 93 | 19 ± 2 | 14 ± 4 | 74 | n/cert | n/d | n/calc | 0.067 ± 0.005 | n/d | n/calc |
| W | n/cert | n/d | n/calc | n/cert | n/d | n/calc | 90 ± 7 | 94 ± 3.2 | 105 | n/cert | n/d | n/calc | n/cert | n/d | n/calc |
| Ba | 430±70 | 440 ± 120 | 103 | 470 ± 60 | 256 ± 45 | 54 | 118 ± 4 | n/d | n/calc | 33.0 ± 2.5 | 26 ± 10 | 79 | 4.8 ± 0.4 | n/d | n/calc |
| Pb | 16 ± 3 | 20 ± 4 | 125 | 16 ± 3 | 14 ± 1 | 88 | 314 ± 13 | 389 ± 26 | 124 | 2.2 ± 0.2 | 2.1 ± 0.9 | 95 | 0.38 ± 0.05 | n/d | n/calc |

[a] This concentration is not detected as the TXRF result is lower than the limit of detection (LOD) value; [b] this value cannot be calculated; [c] this concentration is not certified.

As shown in Table 6, the accuracy of V and Cr determination by TXRF in soil samples does not completely correspond to the requirements [78]. Concentrations of Sr are underestimated but still satisfactory. The accuracy of other elements determination in these soils is quite good for the next ecological monitoring problem. The repeatability values do not exceed 20% for most elements.

A set of elements to be determined by each method was chosen according to previous experience and possibilities of techniques that were developed and applied earlier. WDXRF was used for Na, Mg, Al, Si, P, S, Cl, K, Ca, Ti, Mn, Fe, Br, and Ba determination in pine needles and major oxides ($Na_2O$, MgO, $Al_2O_3$, $SiO_2$, $P_2O_5$, $K_2O$, CaO, $TiO_2$, MnO, and $Fe_2O_3$) determination in soils. TXRF was used for Cr, Ni, Cu, Zn, Rb, Sr, and Pb determination in pine needles and V, Cr, Ni, Cu, Zn, As, Br, Rb, Sr, Y, Ba, and Pb determination in soils.

### *3.2. Distribution of the Elements Examined in Soils and Pine Needles*

Figure 4 shows the ranges of element concentrations in 13 samples of pine needles obtained by the TXRF and WDXRF and the background values [28]. Detailed data are presented in the Supplementary materials, Table S1. The ranges of concentrations are expressed as median, quartiles of 25–75% variation, outliers, and extremes. These outliers and extremes are represented by the values that are "far" from the middle of the distribution. The coefficient of the non-outlier range is equal to one; all these outliers and extremes were determined at 1.5 coefficient. An extreme value was observed at the boundaries of the domain, while an outlier appears to be inconsistent with the remainder of that set of data. Vanadium content in all the measured samples was lower than the LOD value.

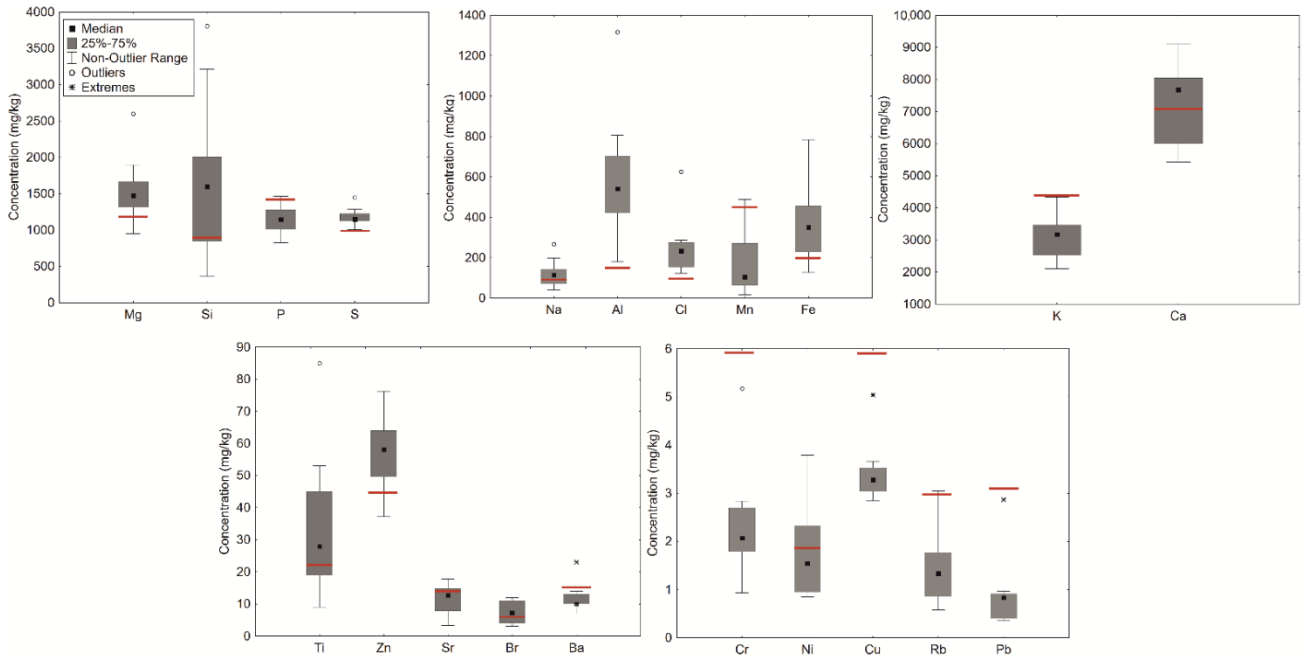


**Figure 4.** The results of pine needle samples analysis by the WDXRF (Na, Mg, Al, Si, P, K, Ca, Ti, Mn, Fe, S, Cl, Br, Ba) and TXRF (Cr, Ni, Cu, Zn, Rb, Sr, Pb) techniques. Note: the red line presents the background values.

As can be seen from the results obtained, the contents of almost all the elements listed in the table are close to the background ones, excluding Zn, Al, Mg, S and Fe. At points located near the quarry (samples 16 and 18), the elevated contents of Si, Al, Fe, and Na are recorded. Excess of the background contents of Al, Fe, Mg, and Cl is observed around the treatment facilities of the IrkAZ (sample 36). The elevated contents of Si, Al, and Na are observed in samples near the smelter (samples 32, 33, 34, and 35). Increased relative to the

background, the Al contents are recorded throughout the entire territory; it must also be said that the specified element is characterized by the maximum values of the excess over the background. High Zn contents can be related to cable production activities.

The trace element composition of studied pine needles samples differs little from the background contents. Ti and Ni have the maximum values of the background excess (2–3 times) in some samples. Ti content prevails in the quarry area (samples 16 and 18) and in the area of the IrkAZ treatment facilities (sample 36). The increased Ni contents are recorded along large highways.

To assess the level of the toxic element concentrations in the examined soils, the maximum permissible concentration values for these elements were taken from the Russian Guide for soil quality [95], and values for Cu from the Canadian Council of Ministers of the Environment (CCME) [96]. The regional background value for As was taken from [97] and, for other elements, from [52]. For pine needles investigation, the regional background values were taken from [28]. Figure 5 shows ranges of the element concentrations in 14 samples of soils obtained by the WDXRF ($Na_2O$, MgO, $Al_2O_3$, $SiO_2$, $P_2O_5$, $K_2O$, CaO, $TiO_2$, MnO, $Fe_2O_3$) and TXRF (V, Cr, Ni, Cu, Zn, As, Br, Rb, Sr, Y, Ba, Pb), the background values, and the maximum permissible concentration values**.** Detailed data are presented in the Supplementary materials, Table S2. W content in all the measured samples was lower than the LOD value.

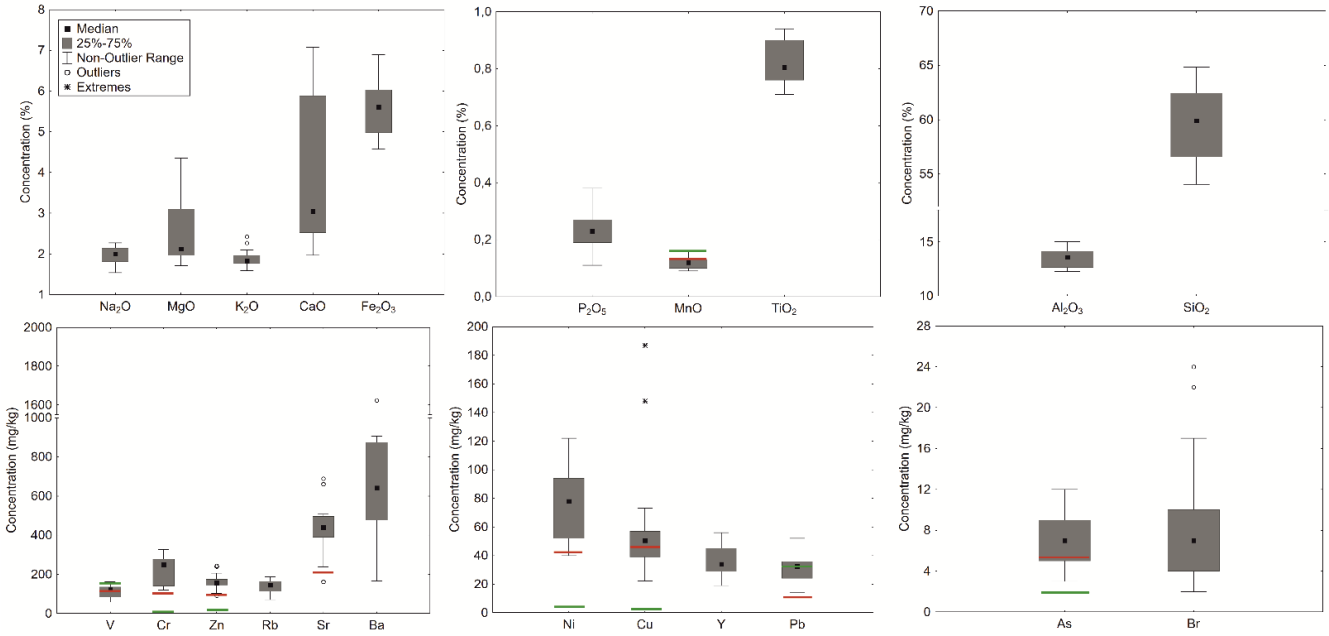


**Figure 5.** The results of the soil samples analysis by the WDXRF ($Na_2O$, MgO, $Al_2O_3$, $SiO_2$, $P_2O_5$, $K_2O$, CaO, $TiO_2$, MnO, $Fe_2O_3$), and TXRF (V, Cr, Ni, Cu, Zn, As, Br, Rb, Sr, Y, Ba, Pb) techniques. Note: The red line presents the background values; green line—maximum permissible concentration.

As can be seen from the results obtained, the contents of many potentially toxic elements (Cr, Zn, Sr, Ni, As, Pb) exceed the background ones. A detailed description of the soil contamination will be expanded further.

All the data were processed using cluster analysis to find correlations (Figure 6).

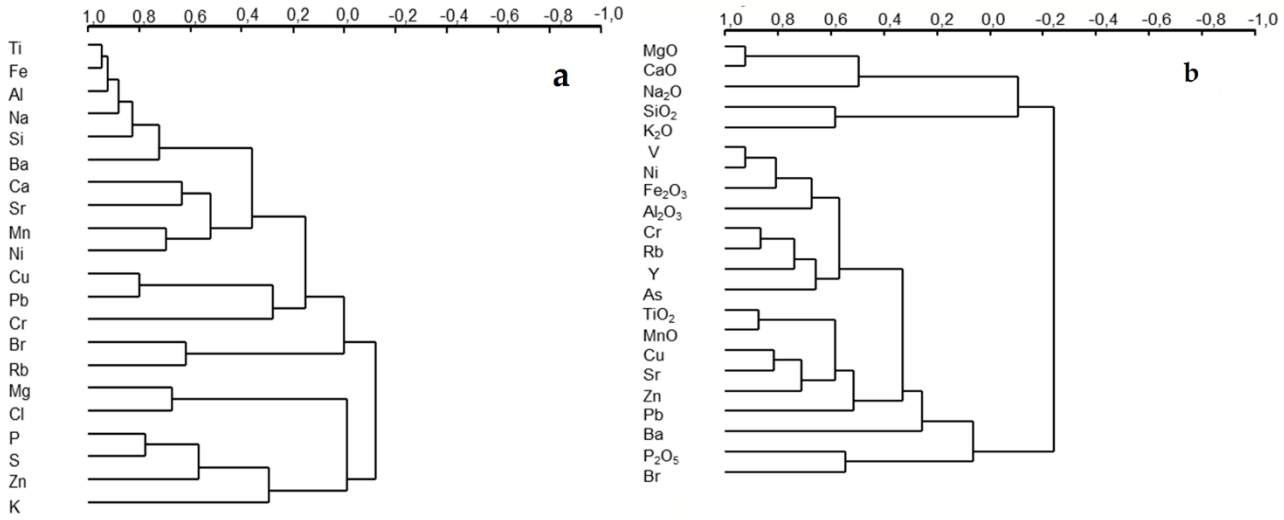


**Figure 6.** The results of cluster analysis of pine needles (a) and soils (b) chemical composition. The upper line is the scale of correlation coefficients between variables and groups of variables.

For pine needles, there is a significant correlation between Fe, Na, Al, Ti, Ba, and Si, which, as has already been noted many times, are one of the main components of gas and dust emissions from the IrkAZ. A high correlation is noted between Mg and Cl. The maximum contents of these elements were detected in the area of the IrkAZ treatment facilities (sample 36). For soils, high correlation coefficients were obtained for MgO and CaO (0.86), which are concentrated in the area of the Maksimovshchina and Smolenschina settlements (samples 1, 6, and 10), as well as for $TiO_2$ and MnO (0.64), concentrated in the Baklashi settlement and the western area of the Shelekhov city (samples 16, 18).

### *3.3. Assessment of the Soil Pollution Level in the Study Area*

The $C_f$ index was studied for each metal in the soil samples. The $C_f$ values were computed using Equation (5). The order of the mean $C_f$ was Pb (3.14) > Cr (2.28) > Sr (2.09) > Zn (1.78) = Ni (1.78) > Cu (1.39) > As (1.21) > V (1.01) > Mn (0.77). High $C_f$ values were observed for Pb (from 3.19 to 5.22) in the soil samples near the treatment facilities of the IrkAZ; 3.34 for Cr in the sample near a motor road, 4.07 for Cu and 3.31 for Sr – near the quarry site, and 3.18 for Sr – from the city area, which give evidence of the contamination level from a moderate to considerable **[86].**

For each toxic element, the EF index was assessed by Equation (6). The mean EF values for the studied area were as follows: Pb (2.81) > Cr (2.03) > Sr (1.85) > Zn (1.59) > Ni (1.56) > Cu (1.19) > As (1.07) > V (0.89) > Mn (0.68). High mean EF values were defined for Cr (2.03) and Pb (2.81), which indicates a moderate enrichment in these soil samples [81]. The maximum values of EF were 4.24 and 4.83 for Pb, which indicates a higher level of pollution. All these samples were collected from the quarry and motor road areas. The mean EF values for Ni, Zn, and Sr vary within the interval of 1.56–1.85, which corresponds to a minimal enrichment in the soil samples examined.

Consistent with Zhang and Liu [90], the values of $0.5 \leq EF \leq 1.5$ denote that the enrichment of trace metal is basically of crustal origin (weathering product), and $EF > 1.5$ suggests that the source of the metal is more anthropogenic. Indeed, the EF values achieved for Cr, Ni, Zn, Pb, and Sr were in the range of 1.56–2.81, which shows a possible anthropogenic origin for these metals.

To assess the overall contamination load for the whole of the studied area, Equation (7) was applied. This assessment indicates a moderate contamination level in the environment according to [91].

The $I_{geo}$ method was applied for the definition of pollution intensity from toxic elements in a given environment [89]. According to Equation (8), the computed $I_{geo}$ values ranged from 0.24 to 1.16 for Cr (mean of 0.53), from 0.10 to 0.84 for Zn (mean of 0.19), from 0.10 to 1.80 for Pb (mean of 1.02), and from 0.33 to 1.14 for Sr (mean of 0.40). This corresponds to small and moderate levels of environmental pollution. Other toxic elements have negative values of the $I_{geo}$ index.

## 4. Conclusions

The WDXRF and TXRF techniques were applied to study the chemical composition of soil and pine needles samples collected in the areas subjected to potential pollution from the aluminum industry and combined heat and power plants. The fusion technique allowed us to quantify major rock-forming elements in soils with good precision, while the method of pressing enabled us to obtain the trace elements in pine needles. The application of the internal standard method made it possible to determine a large set of trace elements in soils and pine needles by TXRF without using external calibration. The XRF results showed a significant level of the several elements concentrations in soils and pine needles, more than doubly exceeding the background values: Na, Mg, Al, Si, Cl, Ti, Fe, Ni, Zn, and Br in pine needles; V, Cr, Ni, Cu, Zn, Rb, Sr, Y, Ba, and Pb in soils. The obtained results indicated a significant pollution level of the studied area. Complex assessment of the soil contamination level using four geochemical indices indicated a pollution level for Pb, Cr, Zn, and Sr from moderate to considerable in the samples collected near the IrkAZ, as well as the quarry site and city area. Moreover, the EF method revealed a possible anthropogenic origin for Cr, Ni, Zn, Pb, and Sr in the soils examined. Investigation of soils and pine needles using XRF techniques is the optimal analytical strategy for the quantitative analysis of natural objects, such as soils and pine needles, and a complementary tool for environmental monitoring.

**Supplementary Materials:** The following are available online at www.mdpi.com/article/10.3390/agronomy12020454/s1: Figure S1: Results of cluster analysis of pine needles' chemical composition. The upper line is the scale of correlation coefficients between variables and groups of variables, Figure S2: Results of cluster analysis of soils chemical composition. The upper line is the scale of correlation coefficients between variables and groups of variables, Table S1: The results of WDXRF and TXRF analysis of pine needle samples (μg/g), Table S2: The results of WDXRF analysis of major oxides (wt. %) and TXRF analysis of microelements (μg/g) in soils samples.

**Author Contributions:** Conceptualization, S.P. and V.C.; methodology, E.C., A.M. and A.A.; formal analysis, E.C., A.M. and A.A.; investigation, S.P. and T.C.; writing—original draft preparation, V.C. and T.C.; writing—review and editing, A.A. and A.M. All authors have read and agreed to the published version of the manuscript.

**Funding:** This work was supported by the governmental assignment of the Vinogradov Institute of Geochemistry SB RAS (projects No. 0284-2021-0003 and 0284-2021-0005), RFBR and the Government of the Irkutsk Region (grant No. 20-45-383003), the Ministry of Science and Higher Education of the Russian Federation (grant No. 075-15-2021-682).

**Data Availability Statement:** The data obtained are available via the author contacts.

**Acknowledgments:** The investigation was carried out using equipment of the SB RAS joint use centers (Geodynamics and Geochronology Center, at the Institute of the Earth's Crust, Siberian Branch of the Russian Academy of Sciences (grant No. 075-15-2021-682); Isotope-geochemical Research Center at the Vinogradov Institute of Geochemistry, Siberian Branch of the Russian Academy of Sciences). The authors kindly acknowledge G.V. Pashkova for helpful advice and discussion of the WDXRF and TXRF results obtained, as well as O.Yu. Belozerova for the EPMA investigation.

**Conflicts of Interest**: The authors declare no conflicts of interest.

## References


1. Revenko, A.G. X-ray fluorescence analysis of rocks, soils and sediments. *X-Ray Spectrom.* **2002**, *31*, 264–273. https://doi.org/10.1002/xrs.564.
2. Potts, P.J.; Webb, P.C.; Watson, J.S. Energy-dispersive X-ray fluorescence analysis of silicate rocks: Comparisons with wavelength-dispersive performance. *Analyst* **1985**, *110*, 507–513. https://doi.org/10.1039/AN985100010.1039/AN9851000507507.
3. Giertych, M.J.; De Temmerman, L.O.; Rachwal, L. Distribution of elements along the length of Scots pine needles in a heavily polluted and a control environment. *Tree Physiol.* **1997**, *17*, 697–703. https://doi.org/10.1093/treephys/17.11.697.
4. Chung, D.; Lee, J.-H.; Lee, S.-Y.; Park, K.-W.; Shim, K.Y. Efficacy of pine needles as bioindicators of air pollution in Incheon, South Korea. *Atmos. Pollut. Res.* **2021**, *12*, 101063. https://doi.org/10.1016/j.apr.2021.101063'
5. Juranović Cindrić, I.; Zeiner, M.; Starčević, A.; Stingeder, G. Metals in pine needles: Characterisation of bio-indicators depending on species. *Int. J. Environ. Sci. Technol*. **2019**, *16*, 4339–4346. https://doi.org/10.1007/s13762-018-2096-x.
6. Pöykiö, R.; Torvela, H. Pine Needles (*Pinus sylvestris*) as a Bioindicator of Sulphur and Heavy Metal Deposition in the Area Around a Pulp and Paper Mill Complex at Kemi, Northern Finland. *Int. J. Environ. Anal. Chem*. **2001**, *79*, 143–154. https://doi.org/10.1080/03067310108035906.
7. Wei, B.; Yang, L. A review of heavy metal contaminations in urban soils, urban road dusts and agricultural soils from China. *Microchem. J.* **2010**. *94*, 99–107.
8. Parzych, A.; Jonczak, J. Pine needles (*Pinus sylvestris* L.) as bioindicators in the assessment of urban environment contamination with heavy metals. *J. Ecol. Eng.* **2014**, *15*, 29–38. https://doi.org/10.12911/22998993.1109119.
9. Shin, J.H.; Yu, J.; Wang, L.; Kim, J.; Koh, S. Investigation of Spectral Variation of Pine Needles as an Indicator of Arsenic Content in Soils. *Minerals* **2019**, *9*, 498. https://doi.org/10.3390/min9080498.
10. Fedotov, P.S.; Dzhenloda, R.K.; Dampilova, B.V.; Doroshkevich, S.G.; Karandashev, V.K. Unexpected behavior of Zn, Cd, Cu, and Pb in soils contaminated by ore processing after 70 years of burial. *Environ. Chem. Lett.* **2018**, *16*, 637–645. https://doi.org/10.1007/s10311-018-0710-2.
11. Kord, B.; Kord, B. Heavy metal levels in pine (*Pinus eldarica* Medw.) tree barks as indicators of atmospheric pollution. *Bioresources* **2011**, *6*, 927–935.
12. Tavares, T.R.; Molin, J.P.; Nunes, L.C.; Wei, M.C.F.; Krug, F.J.; de Carvalho, H.W.P.; Mouazen, A.M. Multi-Sensor Approach for Tropical Soil Fertility Analysis: Comparison of Individual and Combined Performance of VNIR, XRF, and LIBS Spectroscopies. *Agronomy* **2021**, *11*, 1028. https://doi.org/10.3390/agronomy11061028.
13. Menšík, L.; Hlisnikovský, L.; Nerušil, P.; Kunzová, E. Comparison of the Concentration of Risk Elements in Alluvial Soils Determined by pXRF In Situ, in the Laboratory, and by ICP-OES. *Agronomy* **2021**, *11*, 938. https://doi.org/10.3390/agronomy11050938.
14. Lemière, B. A review of pXRF (field portable X-ray fluorescence) applications for applied geochemistry. *J. Geochem. Explor.* **2018**, *188*, 350–363. https://doi.org/10.1016/j.gexplo.2018.02.006.
15. Ravansari, R.; Wilson, S.C.; Tighe, M. Portable X-ray fluorescence for environmental assessment of soils: Not just a point and shoot method. *Environ. Int.* **2020**, *134*, 105250. https://doi.org/10.1016/j.envint.2019.105250.
16. Kalnicky, D.J.; Singhvi, R. Field portable XRF analysis of environmental samples. *J. Hazard. Mater.* **2001**, *83*, 93–122. https://doi.org/10.1016/S0304-3894(00)00330-7.
17. Gutierrez-Gines, M.J.; Pastor, J.; Hernandez, A.J. Assessment of field portable X-ray fluorescence spectrometry for the in situ determination of heavy metals in soils and plants. *Environ. Sci. Process Impacts* **2013**, *15*, 1545–1552. https://doi.org/10.1039/C3EM00078H.
18. Gunicheva, T.N.; Aisueva, T.S.; Afonin, V.P. Non-destructive X-ray fluorescence analysis of soils and friable and marine sediments. *X-Ray Spectrom.* **1995**, *24*, 187–192. https://doi.org/10.1002/xrs.1300240408.
19. Cherkashina, T.Y.; Pellinen, V.A. Applicability of X-ray fluorescence spectrometry for assessing geochemical features and heavy metal contamination of soils: Primary data. *Int. J. Environ. Anal. Chem.* **2020**, *101*, 1–16. https://doi.org/10.1080/03067319.2019.1700971.
20. Cherkashina, T.Y.; Pellinen, V.A. Assessment of soil pollution level using environmental indices in Olkhon Island, Lake Baikal, Russia: Primary data. *Int. J. Environ. Anal. Chem.* **2020**, 1–12. https://doi.org/10.1080/03067319.2020.1759567.
21. Pellinen, V.A.; Cherkashina, T.Y.; Gustaytis, M.A. Assessment of metal pollution and subsequent ecological risk in the coastal zone of the Olkhon Island, Lake Baikal, Russia. *Sci. Tot. Environ.* **2021**, *786*, 147441. https://doi.org/10.1016/j.scitotenv.2021.147441.
22. Pellinen, V.A.; Cherkashina, T.Y.; Ukhova, N.N.; Komarova, A.V. Role of Gravirational Processes in the Migration of Heavy Metals in Soils of the Priolkhonye Mountain-Steppe LandScapes, lake Baikal: Methodology of Research. *Agronomy* **2021**, *11*, 2007. https://doi.org/10.3390/agronomy11102007.
23. Zambello, F.B.; Enzweiler, J. Multi-element analysis of soils and sediments by wavelength-dispersive X-ray fluorescence spectrometry. *J. Soils Sediment*. **2002**, *2*, 29–36. https://doi.org/10.1007/BF02991248.
24. Krishna, A.K.; Murthy, N.N.; Govil, P.K. Multielement Analysis of Soils by Wavelength-Dispersive X-ray Fluorescence Spectrometry. *At. Spectrosc.* **2007**, *28*, 202–214.
25. Belykh, O.A.; Chuparina, E.V.; Mokryy, A.V. Elemental composition of needles of the family pinaceae in the territory with accumulated environmental damage, southern Baikal region. *Russ. J. Gen. Chem.* **2020**, *90*, 2622–2626. https://doi.org/10.1134/S1070363220130150.

26. Belykh, O.A.; Chuparina, E.V. Elemental Composition of Needle Foliage of Pinaceae Forest Forming Species in the Territory with Cumulative Environmental Damage (South Baikal Region). *Bull. Baikal State Univ.* **2021**, *31*, 103–108. https://doi.org/10.17150/2500-2759.2021.31(1).103-108. (in Russian).
27. Chuparina, E.V.; Gunicheva, T.N. Nondestructive x-ray fluorescence determination of some elements in plant materials. *J. Anal. Chem.* **2003**, *58*, 856–861. https://doi.org/10.1023/A:1025689202055.
28. Sanina, N.B.; Filipova, L.A.; Yurkova, I.V.; Chuparina, E.V. Features of the chemical composition of coniferous vegetation of the Priolkhonye. *Geogr. Nat. Resour*. **2008**, *1*, 75–83. (in Russian).
29. Viksna, A.; Selin Lindgren, E.; Standzenieks, P. Analysis of pine needles by XRF scanning techniques. *X-Ray Spectrom.* **2001**, *30*, 260–266. https://doi.org/10.1002/xrs.496.abs.
30. Morgan, T.J.; George, A.; Boulamanti, A.K.; Alvarez, P.; Adanouj, I.; Dean, C.; Vassilev, S.V.; Baxter, D. Quantitative X-ray Fluorescence Analysis of Biomass (Switchgrass, Corn Stover, Eucalyptus, Beech, and Pine Wood) with a Typical Commercial Multi-Element Method on a WD-XRF Spectrometer. *Energy Fuels* **2015**, *29*, 1669–1685. https://doi.org/10.1021/ef502380x.
31. Ichikawa, S.; Nakamura, T. Solid Sample Preparations and Applications for X-Ray Fluorescence Analysis. In *Encyclopedia of Analytical Chemistry*; Meyers, R.A., Ed.; John Wiley and Sons, Inc.: Hoboken, NJ, USA, 2017; pp. 1–22. https://doi.org/10.1002/9780470027318.a9562.
32. Nakayama, K.; Wagatsuma, K. Glass Bead Sample Preparation for XRF. In *Encyclopedia of Analytical Chemistry*; Mayers, R.A., Ed.; John Wiley and Sons, Inc.: Hoboken, NJ, USA, 2017; pp. 1–19. https://doi.org/10.1002/9780470027318.a9632.
33. Klockenkämper, R.; von Bohlen, A. *Total-Reflection X-Ray Fluorescence Analysis and Related Methods*, 2nd ed.; John Wiley and Sons, Inc.: Hoboken, NJ, USA, 2015.
34. Cherkashina, T. Y.; Panteeva, S.V.; Pashkova, G.V. Applicability of direct total reflection X-ray fluorescence spectrometry for multielement analysis of geological and environmental objects. *Spectrochim. Acta B* **2014**, *99*, 59–66. https://doi.org/10.1016/j.sab.2014.05.013.
35. Towett, E.K.; Shepherd, K.D.; Cadisch, G. Quantification of total element concentrations in soils using total X-ray fluorescence spectroscopy (TXRF). *Sci. Total Environ.* **2013**, *463*, 374–388. https://doi.org/10.1016/j.scitotenv.2013.05.068.
36. Towett, E.K.; Shepherd, K.D.; Sila, A.; Aynekulu, E.; Cadisch, G. Mid-infrared and total X-ray fluorescence spectroscopy complementarity for assessment of soil properties. *Soil Sci. Soc. Am. J.* **2015**, *79*, 1375–1385. https://doi.org/10.2136/sssaj2014.11.0458.
37. Park, J.; Park, R.; Han, S.H.; Lim, S.; Lee, C.G.; Song, K. Improvement of accuracy in quantitative TXRF analysis of soil sample by applying external standard method. *Anal. Sci. Technol.* **2016**, *29*, 261–268. https://doi.org/10.5806/AST.2016.29.6.261.
38. Bilo, F.; Borgese, L.; Cazzago, D.; Zacco, A.; Bontempi, E.; Guarneri, R.; Bernardello, M.; Attuati, S.; Lazo, P.; Depero, L.E. TXRF analysis of soils and sediments to assess environmental contamination. *Environ. Sci. Pollut. Res.* **2014**, *21*, 13208–13214. https://doi.org/10.1007/s11356-013-2203-y.
39. Bilo, F.; Borgese, L.; Pardini, G.; Marguí, E.; Zacco, A.; Dalipi, R.; Federici, S.; Bettinelli, M.; Volante, M.; Bontempi, E.; et al. Evaluation of different quantification modes for a simple and reliable determination of Pb, Zn and Cd in soil suspensions by total reflection X-ray fluorescence spectrometry. *J. Anal. At. Spectrom.* **2019**, *34*, 930–939. https://doi.org/10.1039/C9JA00040B.
40. Marguí, E.; Queralt, I.; Hidalgo, M. Application of X-ray fluorescence spectrometry to determination and quantification of metals in vegetal material. *Trends Anal. Chem.* **2009**, *28*, 362–372. https://doi.org/10.1016/j.trac.2008.11.011.
41. De La Calle, I.; Costas, M.; Cabaleiro, N.; Lavilla, I.; Bendicho, S. Fast method for the multielemental analysis of plants and discrimination according to the anatomical part by total reflection X-ray fluorescence spectrometry. *Food Chem.* **2013**, *138*, 234–241. https:doi.org/10.1016/j.foodchem.2012.09.105.
42. Gallardo, H.; Queralt, I.; Tapias, J.; Candela, L.; Margui, E. Bromine and bromide content in soils: Analytical approach from total reflection X-ray fluorescence spectrometry. *Chemosphere* **2016**, *156*, 294–301. https://doi.org/10.1016/j.chemosphere.2016.04.136.
43. Marguí, E.; Floor, G.H.; Hidalgo, M.; Kregsamer, P.; Román-Ross, G.; Streli, C.; Queralt, I. Analytical possibilities of total reflection X-ray spectrometry (TXRF) for trace selenium determination in soils. *Anal. Chem.* **2010**, *82*, 7744–7751. https://doi.org/10.1021/ac101615w.
44. Allegretta, I.; Porfido, C.; Martin, M.; Barberis, E.; Terzano, R.; Spagnuolo, M. Characterization of As-polluted soils by laboratory X-ray-based techniques coupled with sequential extractions and electron microscopy: The case of Crocette gold mine in the Monte Rosa mining district (Italy). *Environ. Sci. Pollut. Res.* **2018**, *25*, 25080–25090. https://doi.org/10.1007/s11356-018-2526-9.
45. Maltsev, A.S.; Chuparina, E.V.; Pashkova, G.V.; Sokol'nikova, J.V.; Zarubina, O.V.; Shuliumova, A.N. Features of sample preparation techniques in the total-reflection X-ray fluorescence analysis of tea leaves. *Food Chem.* **2021**, *343*, 128502. https://doi.org/10.1016/j.foodchem.2020.128502.
46. Bilo, F.; Borgese, L.; Dalipi, R.; Zacco, A.; Federici, S.; Masperi, M.; Leonesio, P.; Bontempi, E.; Depero, L.E. Elemental analysis of tree leaves by total reflection X-ray fluorescence: New approaches for air quality monitoring. *Chemosphere* **2017**, *178*, 504–512. https://doi.org/10.1016/j.chemosphere.2017.03.090.
47. Kumar, R.; Devanathan, A.; Mishra, N.L.; Rai, A.K. Quantification of Heavy Metal Contamination in Soil and Plants Near a Leather Tanning Industrial Area Using Libs and TXRF. *J. Appl. Spectrosc.* **2019**, *86*, 942–947. https://doi.org/10.1007/s10812-019-00919-w.
48. Dalipi, R.; Marguí, E.; Borgese, L.; Depero, L.E. Multi-element analysis of vegetal foodstuff by means of low power total reflection X-ray fluorescence (TXRF) spectrometry. *Food Chem.* **2017**, *218*, 348–355. https://doi.org/10.1016/j.foodchem.2016.09.022.

49. Olsson, M.; Viksna, A.; Helmisaari, H.S. Multi-element analysis of fine roots of Scots pine by total reflection X-ray fluorescence spectrometry. *X-Ray Spectrom.* **1999**, *28*, 335–338. https://doi.org/10.1002/(SICI)1097-4539(199909/10)28:5<335::AID-XRS361>3.0.CO;2-8.
50. Viksna, A.; Znotina, V.; Boman, J. Concentrations of some elements in and on Scots pine needles. *X-Ray Spectrom.* **1999**, *28*, 275–281. https://doi.org/10.1002/(SICI)1097-4539(199907/08)28:4<275::AID-XRS351>3.0.CO;2-C.
51. Grebenshchikova, V.I.; Kuzmin, M.I.; Rukavishnikov, V.S.; Efimova, N.V.; Donskikh, I.V.; Doroshkov, A. Chemical Contamination of Soil on Urban Territories With Aluminum Production in the Baikal Region, Russia. *Air Soil Water Res.* **2021**, *14*, 1–11. https://doi.org/10.1177/11786221211004114.
52. Grebenshchikova, V.I.; Lustenberg, E.E.; Kitayev, N.A.; Lomonosov, I.S. *Geochemistry of the Environment of the Baikal Region (Baikal Geoecological Polygon)*; Academic Publishing House "GEO": Novosibirsk, Russia, 2008; p. 234. (in Russian).
53. Belozertseva, I.A. Chemical element composition of the snow cover in the influence zone of the Irkutsk Aluminum Production Plant. *Geochem. Int.* **2003**, *41*, 614–618.
54. Belykh, L.; Maksimova, M. Eco-Technological Modernization of the Irkutsk Aluminum Plant and its Impact on Carcinogenic Hazard to Shelekhov. *Ecol. Ind. Russ.* **2018**, *22*, 8–13. https://doi.org/10.18412/1816-0395-2018-9-8-13.
55. Belykh, L.I.; Shaimanova, K.A. Sources of carcinogenic risks for atmosphere of Irkutsk Region cities. *IOP Conf. Ser. Mater. Sci. Eng.* **2019**, *687*, 066010. https://doi.org/10.1088/1757-899X/687/6/066010.
56. Belykh, L.I.; Maksimova, M.A. Thermal sources of low power and their caricena hazard to the atmosphere of the cities of the Irkutsk region. *IOP Conf. Series: Earth Environ. Sci.* **2020**, *408*, 012028. https://doi.org/10.1088/1755-1315/408/1/012028.
57. Belogolova, G.A.; Koval, P.V. Environmental geochemical mapping and assessment of anthropogenic chemical changes in the Irkutsk-Shelekhov region, southern Siberia, Russia. *J. Geochem. Explor.* **1995**, *55*, 193–201. https://doi.org/10.1016/0375-6742(95)00016-x.
58. Prosekin, S.N.; Bychinsky, V.A.; Chudnenko, K.V.; Amosova, A.A.; Znamenskaya, T.I. Physicochemical Features of Soil-Forming Processes in Conditions of Technogenic Load. *Geogr. Nat. Res.* **2020**, *41*, 159–165. https://doi.org/10.1134/S1875372820020080.
59. Jarvis, A.; Reuter, H.I.; Nelson, A.; Guevara, E. Hole-Filled Seamless SRTM Data V4, International Centre for Tropical Agriculture (CIAT). 2008. Available online: https://srtm.csi.cgiar.org (accessed on 15 December 2021).
60. Il'in, V.B. *Heavy Metals in Soil-Plant System*; Nauka Press: Novosibirsk, Russia, 1991; p. 151. (in Russian).
61. Kuz'min, V.A. *Soil Geochemistry of the South of the Eastern Siberia*; Geography Institute SB RAS: Irkutsk, Russia, 2005; p. 137. (in Russian).
62. Industrial Standard 41-08-212-04. Quality Control of Analytical Works. 2005. Available online: https://standartgost.ru/g/%D0%9E%D0%A1%D0%A2_41-08-212-04 (accessed on 15 December 2021). (in Russian).
63. Jochum, K.P.; Weis, U.; Schwager. B.; Stoll, B.; Wilson, S.A.; Haug, G.H.; Andreae, M.O.; Enzweiler, J. Reference Values Following ISO Guidelines for Frequently Requested Rock Reference Materials. *Geostand. Geoanalytical Res.* **2015**, *40*, 333–350. https://doi.org/10.1111/j.1751-908X.2015.00392.x.
64. Xie, X.; Yan, M.; Li, L.; Shen, H. Usable Values for Chinese Standard Reference Samples of Stream Sediments, Soils, and Rocks: GSD 9-12, GSS 1-8 and GSR 1-6. *Geostand. Geoanal. Res.* **2007**, *9*. 277–280. https://doi.org/10.1111/j.1751-908X.1985.tb00458.x.
65. Petrov, L.L.; Kornakov, Y.N.; Persikova, L.A.; Anchutina, E.A.; Susloparova, V.E.; Fedorova, I.N.; Shibanov, V.A. Collection of reference samples with composition of natural environments developed at institute of geochemistry. Conditions, problems, prospects. *Anal. Control* **2003**, *7*, 74–82.
**66.** Berkovits, L.A.; Obolyaninova, V.G.; Parshin, A.P.; Romanovskaya, A.R. A System of Sediment Reference Samples: Oo. *Geostand. Newsl.* **1991**, *15*, 85–109. https://doi.org/10.1111/j.1751-908X.1991.tb00099.x.
67. Vazhenin, I.G.; Egorov, V.V.; Lontzikh, S.V.; Shafrinsky, Y.S. Standard samples of soil masses, their preparation and use. *Sov. Soil Sci.* **1977**, *7*, 111–117. (in Russian).
68. Shabanova, E.V.; Vasil'eva, I.E.; Tausenev, D.S.; Scherbarth, S.; Pierau, U. Features of "plants" cluster from the reference materials collection IGC SB RAS. Measurement standards. *Ref. Mater*. **2021**, *17*, 45–61. https://doi.org/10.20915/2687-0886-2021-17-3-45-61. (In Russian).
69. Polkowska-Motrenko, H.; Dybczyński, R.S.; Chajduk, E.; Danko, B.; Kulisa, K.; Samczyński, Z.; Sypuła, M.; Szopa, Z. New Polish certified reference materials for inorganic trace analysis: Corn Flour (INCT-CF-3) and Soya Bean Flour (INCT-SBF-4). *Chem. Analityczna* **2007**, *52*, 361–376.
70. Dybczyński, R.S.; Danko, B.; Kulisa, K.; Maleszewska, E.; Polkowska-Motrenko, H.; Samczyński, Z.; Szopa, Z. Preparation and preliminary certification of two new Polish CRMs for inorganic trace analysis. *J. Radioanal. Nucl. Chem.* **2004**, *259*, 409–413. https://doi.org/10.1023/B:JRNC.0000020909.67144.fc.
71. Shafrinsky, Y.S. Elemental Chemical composition of reference materials of plants. *Sib. Her. Agric. Sci.* **1984**, *83*, 88–55 (in Russian).
72. Certificate of Certified Reference Material human Hair, Bush Twigs and Leaves, Poplar Leaves and Tea (GSV-1,2,3,4 and GSH-1). Institute of Geophysical and Geochemical Exploration. Langfang China, 1990. Available online: https://www.ncrm.org.cn/English/CRM/pdf/GBW07605_20160301_141229758_1692408.pdf (accessed on 15 December 2021).
73. Govindaraju, K. Compilation of Working Value sand Sample Description for 383 Geostandards. *Geostand. Geoanalyt. Res.* **1994**, *18*, 1–158. https://doi.org/10.1046/j.1365-2494.1998.53202081.x-i1.
74. Jochum, K.P.; Nohl, U.; Herwig, K.; Lammel, E.; Stoll, B.; Hoffman, A.W. GeoReM: A New Geochemical Database for Reference Materials and Isotopic Standards. *Geostand. Geoanal. Res.* **2005**, *29*, 333–338. https://doi.org/10.1111/j.1751-908X.2005.tb00904.x.
75. *SPECTRA*$^{plus}$, version 2.2.3.1.; Software Package for X-Ray Spectrometers; Bruker AXS GmbH: Karlsruhe, Germany, 2008.

76. Amosova, A.A.; Panteeva, S.V.; Tatarinov, V.V.; Chubarov, V.M.; Finkelshtein, A.L. X-ray fluorescence determination of major rock forming elements in small samples 50 and 110 mg. *Anal. Control* **2015**, *19*, 130–138. https://doi.org/10.15826/analitika.2015.19.2.009. (In Russian).
77. Magnusson, B.; Örnemark, U. *Eurachem Guide: The Fitness for Purpose of Analytical Methods—A Laboratory Guide to Method Validation and Related Topics*, 2nd ed.; Eurachem Press: London, UK; 2014; p. 70.
78. Barwick, V. *Eurachem/CITAC Guide: Guide to Quality in Analytical Chemistry: An Aid to Accreditation*, 3rd ed.; CITAC: London, UK; 2016; p. 66.
79. *SPECTRA*, version 7.8.2.; Software Package for TXRF Spectrometers; Bruker AXS Microanalysis GmbH: Berlin, Germany, 2007.
80. Wei, B.; Jiang, F.; Li, X.; Mu, S. Spatial distribution and contamination assessment of heavy metals in urban road dusts from Urumgi, NW China. *Microchem. J.* **2009**, *93*, 147–152. https://doi.org/10.1016/j.microc.2009.06.001.
81. Sutherland, R.A. Bed sediment-associated trace metals in an urban stream, Oahu, Havaii. *Environ. Geol.* **2000**, *39*, 611–627. https://doi.org/10.1007/s002540050473.
82. Magiera, T.; Zawadzki, J.; Szuszkiewicz, M.; Fabijanczyk, P.; Steinnes, E.; Fabian, K.; Miszczak, E. Impact of an iron and a nickel smelter at the Norwegian/Russian border close to the Barents Sea on surface soil magnetic susceptibility and content of potentially toxic elements. *Chemosphere* 2018, *195*, 48–62. https://doi.org/10.1016/j.chemosphere.2017.12.060.
83. World Health Organization Classifications, IARC, 2018. Available online: https://monographs.iarc.who.int/list-of-classifications/ (accessed on 15 December 2021).
84. Lin, Y.; Meng, F.; Du, Y.; Tan, Y. Distribution, speciation, and ecological risk assessment of heavy metals in surface sediments of Jiaozhou Bay, China. *Hum. Ecol. Risk. Assess.* 2016. *22*, 1253–1267. https://doi.org/10.1080/10807039.2016.1159503.
85. Saraee, K.R.E.; Abdi, M.R.; Naghavi, K.; Saion, E.; Shafaei, M.A.; Soltani, N. Distribution of heavy metals in surface sediments from the South China Sea ecosystem. Malaysia. *Environ. Monit. Assess.* **2011**, *183*, 545–554. https://doi.org/10.1007/s10661-011-1939-4.
86. Hakanson, L. An ecological risk index for aquatic pollution control. A sedimentological approach. *Water Res.* **1980**, *14*, 975–1001. https://doi.org/10.1016/0043-1354(80)90143-8.
87. El Zrelli, R.; Courjault-Rade, P.; Rabaoui, L.; Castet, S.; Michel, S.; Bejaoui, N. Heavy metal contamination and ecological risk assessment in the surface sediments of the coastal area surrounding the industrial complex of Gabes city, Gulf of Gabes, SE Tunisia. *Mar. Pollut. Bull.* **2015**, *101*, 922–929.
88. Simex, S.A.; Helz, G.R. Regional geochemistry of trace elements in Checapeake Bay. *Environ. Geol.* **1981**, *3*, 315–323. https://doi.org/10.1007/BF02473521.
89. Ergin, M.; Saydam, C.; Basturk, O.; Erdem, E.; Yoruk, R. Heavy metal concentrations in surface sediments from the two coastal inlets (Golden Horn Estuary and Izmit Bay) of the northeastern Sea of Marmara. *Chem. Geol.* **1991**, *91*, 269–285. https://doi.org/10.1016/0009-2541(91)90004-B.
90. Zhang, J.; Liu, C.L. Riverine composition and estuarine geochemistry of particulate metals in China—Weathering features, anthropogenic impact and chemical fluxes. *Estuar. Coast Shelf Sci.* **2002**, *54*, 1051–1070. https://doi.org/10.1006/ecss.2001.0879.
91. Tomlinson, D.L.; Wilson, J.G.; Harris, C.R.; Jeffrey, D.W. Problems in the assessment of heavy-metal levels in estuaries and the formation of a pollution index. *Helgol. Mar. Res.* **1980**, *33*, 566–575. https://doi.org/10.1007/BF02414780.
92. Liu, G.; Tao, L.; Liu, X.; Hou, J.; Wang, A.; Li, R. Heavy metal speciation and pollution of agricultural soils along Jishui River in non-ferrous metal mine area in Jiangxi Province, China. *J. Geochem. Explor*. **2013**, *132*, 156–163. https://doi.org/10.1016/j.gexplo.2013.06.017.
93. Muller, G. Index of geo-accumulation in sediments of the Rhine River. *Geojournal* **1969**, *2*, 108–118.
94. Yaqin, J.I.; Yinchang, F.E.N.G.; Jianhui, W.U.; Tan, Z.H.U.; Zhipeng, B.A.I.; Chiqing, D.U.A.N. Using geoaccumulation index to study sources profiles of soil dusts in China. *J. Environ. Sci.* **2008**, *20*, 571–578. https://doi.org/10.1016/S1001-0742(08)62096-3.
95. Onishchenko, G.G. Maximum Permissible Concentrations (MACs) of Chemicals in Soil: Hygienic Standards 2.1.7.2042-06 Federal Center for Hygiene and Epidemiology of Rospotrebnadzor, Moscow, 2006. Available online: https://files.stroyinf.ru/Data2/1/4293850/4293850510.htm (accessed on 15 December 2021).
96. CCME, Canadian Council of Ministers of the Environment. Canadian Soil Quality Guidelines for the Protection of Environmental and Human Health. 2017. Available online: http://esdat.net/Environmental%20Standards/Canada/SOIL/rev_soil_summary_tbl_7.0_e.pdf (accessed on 15 December 2021).
97. Letter from the Ministry of Natural Resources of the Russian Federation No. 04-25, Roskomzem No. 61-5678 from 27.12.1993. On the procedure for determining the amount of damage from land pollution by chemical substances. Available online: http://www.referent.ru/1/6352 (accessed on 15 December 2021).